Line Voltages THD Optimization on a Multilevel Inverter for PV Systems

LUIS DAVID PABON, JORGE LUIS DIAZ RODRIGUEZ, ALDO PARDO GARCIA.
Department of Electrical Engineering and Mechatronics
University of Pamplona
Ciudadela Universitaria, Km 1 via Bucaramanga, Pamplona
COLOMBIA
davidpabon@unipamplona.edu.co, jdiazcu@unipamplona.edu.co , apardo13@unipamplona.edu.co

Abstract: - This paper presents the optimization of total harmonic distortion (THD) applied directly to the line voltages output from a multilevel power inverter, with H-bridges cascaded common source of nine steps per phase applied to a photovoltaic system. The mathematical model of the THD of line voltages is presented in terms of commutation angles of the PWM phase modulation following the IEEE-519 standard. This equation gives a new and purely numerical optimization character, allowing to obtain excellent results using genetic algorithms reaching a THD of 0.3% in line voltages. To validate the results obtained by mathematical modeling and optimization, an algorithm using the FPGA Virtex5 XUPV5-LX110T is implemented.

Key-Words: - Three-phase multilevel power inverter, multilevel PWM modulation, H-bridges cascaded common source, THD, Genetic algorithm, Optimization.

1. Introduction

Currently there is a pronounced interest at generating high quality electricity, through alternative energy sources, this is due to environmental disasters caused by many factors, one of them is the conventional sources of energy, in this context solar energy has been widely accepted because of its many advantages as a source of renewable energy and has presented a continuous growth in recent years [1], settling large number of photovoltaic systems around the world [2].

The production of electricity from solar panels is given in direct component, using power inverters is a complete solution to convert AC voltage output [3] for the use of energy or connecting to the power network [2]. However, conventional converters used in this application have certain problems in terms of power quality, due to harmonic distortion [4], [5].

Since in photovoltaic (PV) systems into alternating the power quality depends on the power inverter [6], today there have been numerous investigations aimed on optimizing the harmonic content of these [7], [8], presenting multilevel converters as a solution to the problem, because these inverters have many advantages compared with conventional two levels: waveforms of high quality energy, low loss switching capacity of high voltage, low electromagnetic interference, etc. [9]-[11]. In this way exclusive area harmonic content optimization of photovoltaic systems through multilevel converters works are presented [12] - [14].

This research through using genetic algorithms aims to optimize the harmonic content of the three phase photovoltaic systems, minimizing THD line directly through a cascaded asymmetric H-bridge common source multilevel power converter [15] nine levels phase adopt the modulation found by the optimization algorithm.

2. State of The Art

The multilevel power converter appears in the year 1975 with Baker and Lawrence patent [16], performing the first implementation in 1981 [17], from these works, numerous investigations have come to get a variety of converters [11] some of which are considered as classics [3]: fixing converters diodes, capacitors and floating H-bridges cascade. In the same way recently topologies that are considered innovative and seek to reduce the number of components, increase efficiency or improve power quality have appeared [18]-[20].

Inside the classic topologies, the cascade H-bridges is considered advantageous in terms of quality of the waveform and number of components [3], within this a convenient sub-topology appears in photovoltaic systems using an accumulator block, because it uses a single voltage source directly, accompanied by a transformer at the output of the

H-bridge, this topology is named as a multilevel converter cascaded H-bridge common source [21]. This configuration is very suitable for low cost renewable energy applications, because it feeds the entire system from a single source [9] however, using a transformer to the output, creates problems in terms of the perturbation of the waveform and makes the system even more complex [9], [22]. Problems have been studied and have been solved in works like [6] and [23].

In the field of optimization of the harmonic content of the modulations of multilevel converters there have been numerous proposed techniques depending on the topology used, the specific objective and the shape of the search for an optimum [24], [25], however there are very promising strategies in the line of evolutionary algorithms and particle swarm (PSO) and genetic algorithms (GA) [8], some of these studies conclude that outperforms genetic algorithms [8] and [26].

Similarly these optimizations mostly made in the phase voltages of the converters [15], [28], [29] and very few are made directly in the line voltages [30] reaching results not so near from zero. For these reasons in this paper a multilevel converter H-bridges common source cascade that optimizes THD of line voltages directly, using genetic algorithms, as proposed to improve power quality three-phase PV systems is presented.

3. Cascade Multilevel Converter Phase of Common source of Nine Steps for Phase

The topology of multilevel inverter selected for this work is the inverter H-bridge asymmetrical cascade common source with 1: 3 ratio of 2 stages, which generates 9 levels of output voltage of each phase, this topology is shown in Figure 1.

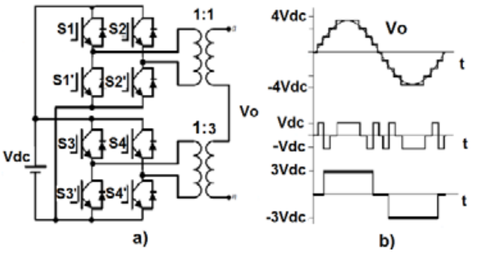

Fig. 1. Asymmetry Cascade Inverter in common source of two stages with 9 levels at the output, asymmetry. 1: 3 Topology. b) Vo.

This converter allows a minimum of stages of H-bridges (2 steps) to achieve the possible maximum number of output voltage steps (9 steps). The Figure 2 shows the three-phase topology, which is nothing but the triplication of the single phase presented in Figure 1. As shown, the three phases share the DC bus.

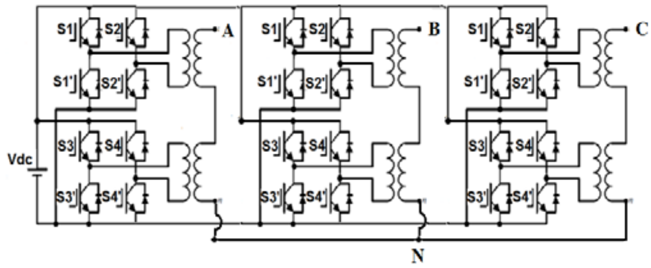

Fig. 2. Converter topology.

The waveform generated by the phase converter shown in Figure 3. This voltage waveform is achieved if phase-multilevel PWM modulation is generated. It is expected that the line voltage converter has more steps and more pulses due to the subtraction between phase voltages, this will be shown in later sections.

4. Mathematical modeling

In this study obtained an expression that quantifies the total harmonic distortion of line voltages in terms of commutation angles of each step of the phase voltage, both on and off angles.

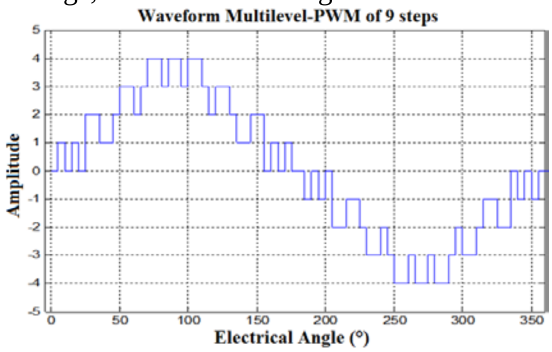

Fig. 3. PWM modulation waveform of 9 steps per phase.

In order to determine this equation it was modeled using Fourier phase voltages A and B series of an ABC phase system of nine steps PWM modulations, and since the line voltage is the subtraction of the phase voltages (on a connection and for the converter), the Fourier series of the line voltage is obtained by the respective difference. Getting the Fourier series of line voltage THD is calculated in terms of the first 50 harmonics following the IEEE 519 standard [31].

Phase A

As the shape of the modulation shown in a quarter (1/4) guarding symmetry wave, it is only necessary to define the firing angles in the first quarter wave (Fig. 4), the remaining parts of the modulation are constructed using trigonometric relationships. Thus a vector $L = [a\ b\ c\ d]$ representing the total number of switch on and switch off angles at each step is established. The Fourier series for periodic waveforms states:

$$v(t)=\frac{a_0}{2}+\sum_{n=1}^{\alpha}\left(a_n\cos n\omega_0 t+b_n\sin n\omega_0 t\right) \quad (1)$$

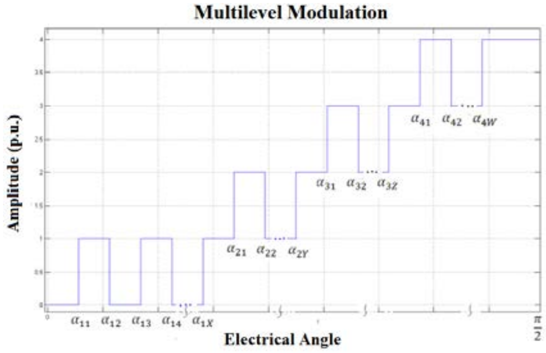

Fig. 4. A quarter of a modulation waveform in terms of switch on and switch off of each step angles.

Where n is the harmonic number, w_o the fundamental frequency wave, time t, $a_0/2$ is the DC component, which is calculated by the expression:

$$a_0=\frac{1}{2\pi}\int_0^{2\pi}v(\omega t)\,d(\omega t) \quad (2)$$

a_n coefficient of the Fourier series is calculated with (3): $a_n=\frac{1}{\pi}\int_0^{2\pi}v(\omega t)\cos n(\omega_0 t)\,d(\omega t)$ (3)

b_n coefficient of the Fourier series, calculated by:

$$b_n=\frac{1}{\pi}\int_0^{2\pi}v(\omega t)\sin n(\omega_0 t)\,d(\omega t) \quad (4)$$

The waveform (Fig. 4) presents uneven symmetry and the positive part is equal to the negative applying thereby, symmetries as the theory of Fourier series.

$$a_o=0 \text{ and } a_n=0 \quad (5)$$

Only the coefficient related within the sinus will remain, therefore the waveform in terms of the Fourier series, will be expressed as follows:

$$v(t)=\sum_{n=1}^{\alpha}b_n\sin n\omega_0 t \quad (6)$$

b_n in terms of L vector for waveform:

$$b_n=\frac{4v_{cd}}{n\pi}\left[\sum_{i=1}^{4}\sum_{j=1}^{L_i}(-1)^{j-1}\cos n\alpha_{ij}\right] \text{ for odd } n; \quad (7)$$

y $b_n=0$ for even n.

Where i is the number of the step (hence the sum is from 1 to 4), L_i the vector's i component L and α_{ij} the j angle of the i step, this can be switch on or switch off. For a ladder vector components L must be odd. If the peak magnitude of harmonic n, in the Fourier series is defined as:

$$h_n=\sqrt{a_n^2+b_n^2} \quad (8)$$

Substituting (5) and (7) (8) the peak magnitude of each harmonic n, where only odd harmonics will exist because b_n=0, if n is even therefore obtained as:

$$h_n=\frac{4v_{cd}}{n\pi}\left[\sum_{i=1}^{4}\sum_{j=1}^{L_i}(-1)^{j-1}\cos n\alpha_{ij}\right] \text{ for } n = 1, 3, ..., \quad (9)$$

The expression in the form of Fourier series phasors of a waveform in terms of the fundamental and harmonic component:

$$v(t)=a_0+\sum_{n=1}^{\alpha}h_n\sin(n\omega t+\varphi_n) \quad (10)$$

Where a_0 is the direct component, h_n the amplitude for each harmonic calculated in (9) and φ_n the phase of each harmonic calculated in (11):

$$\varphi_n=\tan^{-1}\frac{a_n}{b_n} \quad (11)$$

For this case φ_n and null a_0 and therefore the associated terms for the Fourier series for phase A, in the form of equation (10), are:

$$h_n=\begin{cases}0 & \text{for even } n\\ \frac{4v_{dc}}{\pi n}\sum_{i=1}^{4}\sum_{j=1}^{L_i}(-1)^{j-1}\cos n\alpha_{ij} & \text{for odd } n\end{cases} \quad (12)$$

$$\varphi_n=0 \quad (13)$$

Phase B

Determining the Fourier series of phase B of the ABC system, the *A* waveform from Fig. 3 was offset. 120° in arrears, this corresponds to each angle presented in Fig. 4 should be shifted $2\pi/3$ rad, and due to this displacement the odd symmetry is not applicable to this waveform, thus following the same process of A phase it is possible to calculate the Fourier series of the phase B but in this case should be calculated on the a_n and b_n full cycle.

The shifted phase wave form still has symmetry about the x-axis component thus direct voltage remains null Phase *B*:

$$a_o=0 \quad (14)$$

The terms associated for the Fourier series for phase B, in the form of equation (10), are those shown in (15) and (16):

$$C_n=\begin{cases}0 & \text{for even } n\\ \frac{4v_{dc}}{\pi n}\left(\sum_{i=2}^{4}\sum_{j=2}^{L_i}(-1)^{j-1}\cos n\alpha_{ij}\right) & \text{for odd } n \text{ (multiple of 3)}\\ \frac{4v_{dc}}{\pi n}\left(\sum_{i=2}^{4}\sum_{j=2}^{L_i}(-1)^{j-1}\cos n\alpha_{ij}\right) & \text{for odd } n \text{ (non multiple of 3)}\end{cases} \quad (15)$$

k represents the number of odd harmonic not multiple of 3, for example k=1, n=5, k=2 to n=7, k=3 to n=11, so on.

Line Voltage

For calculating the Fourier series in the line voltages set out from the Fourier series of the voltages phase difference:

$$v_{AB}(t) = v_A(t) - v_B(t) \tag{16}$$

By making the respective differences of the Fourier series of Phases A and B, in the forms of equation (10) with the amplitudes and offsets given by (12), (13), (15) and (16) the Fourier series for v_{AB} line voltage is obtained, but in the article only the harmonic amplitude is presented, since the objective is to minimize THD and for this mismatch harmonics are required, therefore the harmonic amplitudes of the line voltages shall be expressed by equation (17)

$$h_n = \begin{cases} 0 & \text{for even } n \\ 0 & \text{for odd } n \text{ (multiple of 3)} \\ \dfrac{4\sqrt{3}v_{dc}}{\pi n}\left(\sum_{i=2}^{4}\sum_{j=2}^{L_i}(-1)^{j-1}\cos n\alpha_{ij}\right) & \text{for odd } n \text{ (non multiple of 3)} \end{cases} \tag{17}$$

THD of line voltage

The IEEE 519 standard in 1992 on page 63 [31] defines the total harmonic distortion as equation10:

$$THD = \frac{\sqrt{\sum_{n=2}^{50} h_n^2}}{h_1} \cdot 100 \tag{18}$$

Where h1 is the fundamental harmonic component and h_n the peak of the harmonic n. Replacing (17) in (18):

$$THD = \frac{\sqrt{\sum_{n=2}^{50}\left(\frac{1}{n}\left[\sum_{i=1}^{4}\sum_{j=1}^{L_i}(-1)^{j-1}\cos n\alpha_{ij}\right]\right)}}{\sum_{i=1}^{4}\sum_{j=1}^{L_i}(-1)^{j-1}\cos n\alpha_{ij}} \cdot 100\% \tag{19}$$

Where n takes not odd values non multiple of 3, i.e. 5, 7, 11, 13, 17, etc. and L_i are the components of the vector $L = [a\ b\ c\ d]$. Thus (19) defines the objective function to be minimized by the optimization algorithm.

5. Optimization Algorithm

With the help of Matlab® and *GA* command (Genetic Algorithm) algorithms for the mathematical model of the fitness function (Equation 19) and its respective optimization using genetic algorithms were programmed. The size of the population for the algorithm is taken from 20 individuals, each individual (X) consists of the total of shooting angles in the first wave quarter:

$$X = \left[\alpha_{11}\alpha_{12}\cdots\alpha_{1x}\alpha_{21}\alpha_{22}\cdots\alpha_{2y}\alpha_{31}\cdots\alpha_{3z}\alpha_{11}\cdots\alpha_{1w}\right] \tag{20}$$

Accompanied by the L vector indicating the program responsible for evaluating the fitness function angles corresponding to each step. The flowchart of the algorithm shown in Fig. 5.

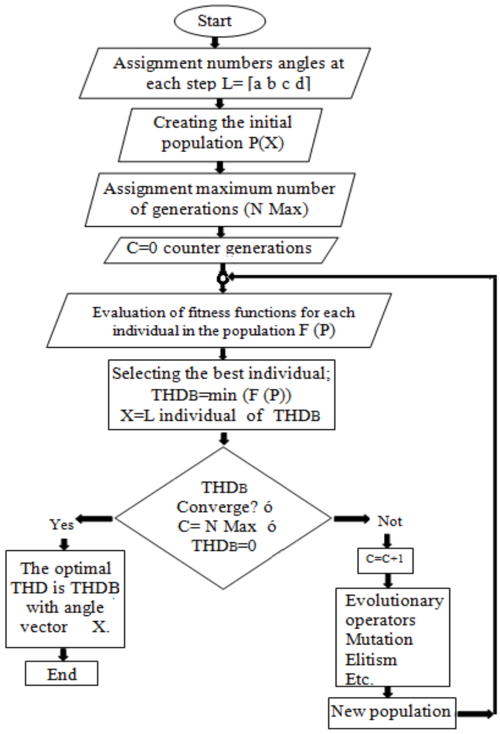

Fig. 5. Flowchart of the optimization algorithm (GA).

6. Results

$L = [3\ 3\ 5\ 9]$ is the vector which defines the number of firing angles in each step indicating that the first and second step have a pulse and a half, in the third step two pulses and a half, in the last step 4 pulses and a half in the first quarter wave voltage phase. Firing angles of phase are summarized in Table I

TABLE I: ANGLES IN DEGREES OF THE BEST INDIVIDUAL.

a=3	b=3	c=5	d=9	
5.70241538	18.229993	34.4310184	53.386964	73.2043847
9.94093425	24.218687	34.7242607	55.288426	73.2387503
12.51467958	26.1824422	36.5706369	60.479581	78.4542332
		45.0850569	64.6966	81.6462089
		47.1467285	67.878653	

The THDv of line voltages of a balanced three-phase system which uses a nine steps phase modulation with shooting previous fire angles theoretically will be of 0.000132%. THDv introduced a phase of 10.8631%. In Figure 6 the v_A waveform voltage phase is shown, and in Figure 6.b its harmonic spectrum.

Figure 6, b shows that the harmonics appearing in the phase modulation are tripling, because of this the THD phase is high (10.8631%), these harmonics are deleted in the line voltage at withdrawing the two positive sequence phases. The waveforms of three-phase line modulations obtained by subtracting the phases of the positive sequence waveforms is shown in Figure 6, shown in Figure 7.a and its spectrum is shown in Figure 7.b.

As shown in Figure 7.a, there in the line voltage appear additional steps due to the subtraction done between the phases, phase modulation has nine steps, while the line has 15 steps, similarly more pulses occur, and this makes the waveform get closer to the sinusoidal and therefore the harmonic content decreases reaching a value of 0.000132%.

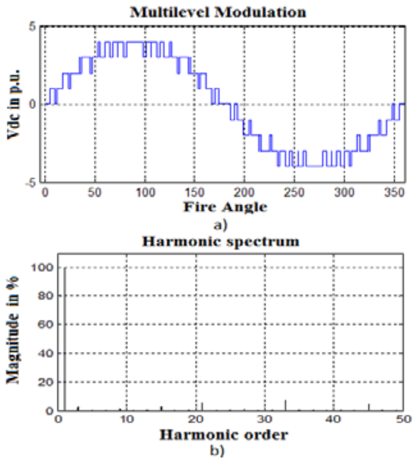

Fig. 6. Phase modulation. a) Waveform. b) Harmonic spectrum.

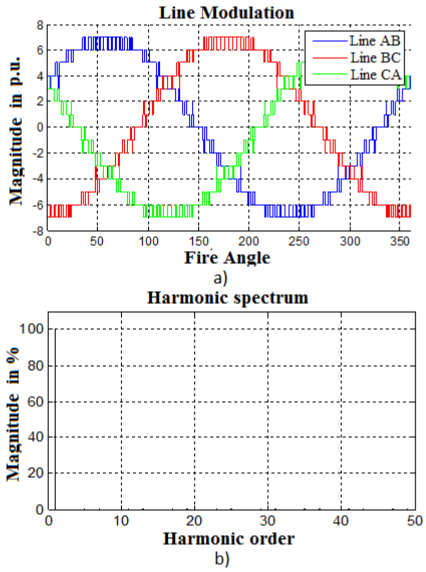

Fig. 7. Line Modulation. a) Waveform. b) Harmonic spectrum.

7. Implementation

In order to validate, a three-phase inverter prototype was implemented according to the topology selected in section III, based on the use of MOSFETs as switching devices. The power converter is rated 2100 VA, the input voltage 48 V_{dc}, aimed to be applicable to low cost photovoltaic systems in which only an accumulator block for this voltage is taken, the 60 Hz nominal frequency, and a nominal output voltage of 127 Vrms and 220 Vrms phase line. The control of converter is performed only with twelve signals, necessary to control the upper MOSFETs of the bridges, the lower is controlled by the denial of the 12 signs of major control and allocation of downtime was made along with the denial through hardware.

The control device in the experimental stage was based on the use of FPGAXUPV5-LX110T. The design of transformers, critical devices in achieving the waveform, raised according to the methodology proposed in [23]. The implemented prototype is shown in Figure 8.

8. Experimental Test

Figure 8 shows assembly for the experimental tests carried out, here is possible to observe the basic components of the inverter: H-bridges, transformers, driver stage and FPGA. The analyzer power quality Fluke 434 and the 125 Fluke oscilloscope: the accumulator block, represented by laboratory sources from which the drive and measuring equipment are fed is also observed.

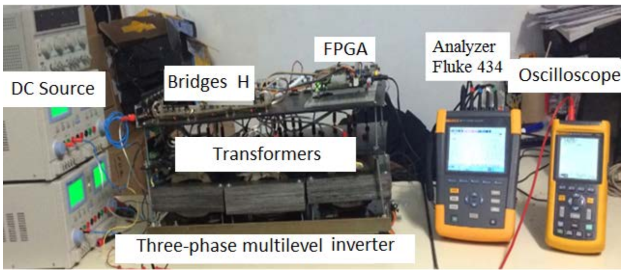

Fig. 8. Mounting experimental tests with FPGA.

With the above assembly waveforms, RMS values, THD, phasor diagrams of the phase voltages and line, as the output currents of the inverter, for testing in vacuum, resistive load (resistive bank 250 W) were observed, inductive load (induction motor 1 Hp) and capacitive load (250W and 150 VAR), in order to validate the harmonic content of the implemented modulations.

Figure 9.a shows the waveform of the line voltages empty converter, with the spectrum given by the analyzer (figure 9.b This figure was expanded showing the ordinate axis with 20% encouragement of evidence that there is no harmonic), also, the spectrum of the phase voltage is presented to show the presence of harmonics in the phase and demonstrate effectively that optimization is done directly online.

In Figure 9.a. all pulses are not seen due to the display resolution of the analyzer, Figure 10.a shows the shape of the waveform of the line voltage captured on the oscilloscope in which the presence of all pulses is observed and in figure 10.b the phasor diagram of the voltages and currents for inductive load test shows the accuracy gaps and the system frequency are evident. In Figure 10.c spectrum is shown to the three line voltages, which shows the replica of behavior in the three line voltages.

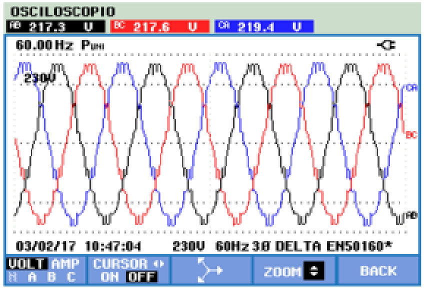

a)

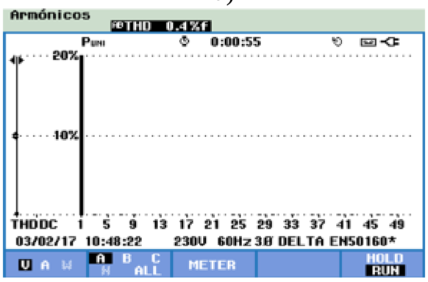

b)

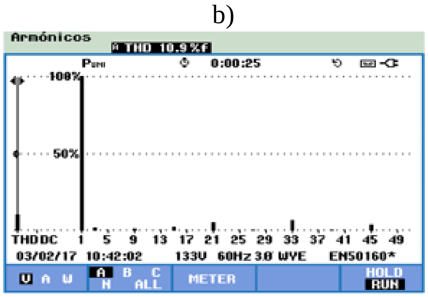

c)

Fig. 9. a) Line voltage waveform. b) Spectrum. c) Spectrum of the phase voltage.

A consolidate of all the tests is shown in Table II, factor imbalance and percent control are calculated as presented in [31]. This table shows that the THD of the phase voltages is quite high in all tests, but the THD of line that is optimized in that work oscillates at very low values of 0.3-0.6%.

a)

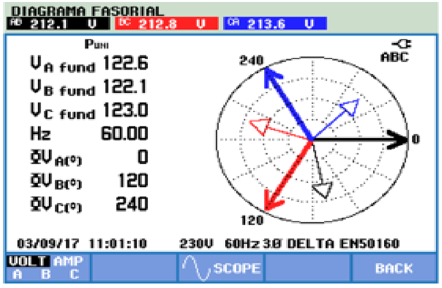

b)

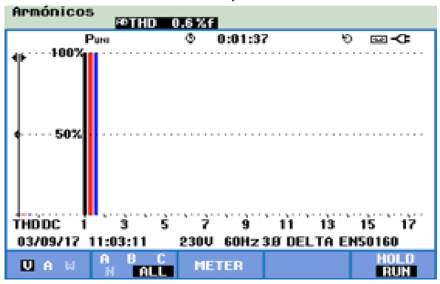

c)

Fig. 10. a) Waveform line voltage. b) Phasor diagram. c) Line voltages spectrum in the inductive test.

TABLE II: Consolidated tests results.

Variable	Parameter	Test			
		Non load	Resist.	Induc.	Capac.
Phase Voltage	Mean Vrms (V)	126.23	120.33	123.73	120.67
	% Regulation	0	4.67	1.97	4.4
	% Unbalance factor	1.28	1.27	1.15	0.63
	%THDv	10,9	11.6	11.2	11.5
Line Voltage.	Mean Vrms (V)	218.1	206.86	212.86	206.96
	% Regulation	0	5.15	2.3	5.1
	% Unbalance factor	0.59	0.64	0.34	0.59
	%THDv	0.4	0.3	0.6	0.3
Line Current.	Mean Irms (A)	0	0.716	1.08	0.81
	% Unbalance factor	0	0.41	2.68	0.2
	$\%THD_I$	0	0.5	2.3	0.9
Power	Output Power (W)	0	255.1	86.7	256
	Power Factor	0	1	0.22 L	0.88 C
	Reactive Power(VA)	0	255.1	397	291

Likewise, it is observed that the imbalances in the phase voltages and line meets EN50160 which establishes a maximum of 2%, as percentages of regulation which is maintained within the range established by the IEEE 1159 which states that the normal band operation voltage must be within 10% fluctuation.

9. Conclusions

The phase voltage THD in this work is quite high because the proposed optimization is directly in line voltages. The value of THDv phase ranged from 10.9% in the vacuum test and 11.6% in the test resistive load. This shows that the load disturbs the behavior of the converter; however variations are not very representative. As for the measured harmonic spectra phase voltages each of the tests demonstrated that the components present were triples because as deduced in mathematical modeling these harmonics would be eliminated in the line voltages by the potential difference between the two phases.

THD of line voltages evidences good optimization performed by the algorithm, since all THD tests were below the limit set by the IEEE 519 which is 5%. It presenting the highest THD at a value of 0.6%, which is a very low value.

The results regarding the THDv voltage line reflects the good design of the converter, as this reproduces the waveforms calculated in an accurate manner, although the converter uses transformers; the same design minimizes perturbations they could generate, is for this reason that the THD is very low despite the presence thereof.

The optimization algorithm developed will be able to override all defined harmonic content between 2 and 50 if a sufficient number of shooting angles is given, however, modulations that are not possible to implement can occur.

The optimized theoretician THD of this project is defined as 0.2207% that this is the harmonic content of the modulation optimized to the 50th harmonic, being the upper bound of evaluation established by the IEEE 519 on page 63.

From the experimental point of view the optimized THD for line voltage waveform is defined as 0.6% because this is the largest THD present in the tests.

The converter meets the quality standards of energy; this is why this converter is a good proposal to improve the quality of three-phase PV energy systems.

References

[1]. Mohammad Barghi Latran, Ahmet Teke, Investigation of multilevel multifunctional grid connected inverter topologies and control strategies used in photovoltaic systems, Renewable and Sustainable Energy Reviews, Volume 42, February 2015, Pages 361-376, ISSN: 1364-0321.

[2]. P. Veena, V. Indragandhi, R. Jeyabharath, V. Subramaniyaswamy, Review of grid integration schemes for renewable power generation system, Renewable and Sustainable Energy Reviews, Volume 34, June 2014, Pages 628-641, ISSN: 1364-0321.

[3]. [3] Abdelaziz Fri, Rachid El Bachtiri, Abdelaziz El Ghzizal, A Comparative Study of Three Topologies of Three-phase (5L) Inverter for a PV System, Energy Procedia, Volume 42, 2013, Pages 436-445, ISSN 1876-6102.

[4]. Mohammad, S. Z.; Omar, A. N. and Ibrahim, I. R. “A Review of Single-Phase Single Stage Inverter Topologies for Photovoltaic System”. 4th Control and System Graduate Research Colloquium, Shah Alam, Malaysia, Vol. 19, N. 20, Aug. 2013, pp. 69-75.

[5]. Mehmet, Y.; Seydi, V.; Seci, V. and Hasan, C. “Comparison of Output Current Harmonics of Voltage Source Inverter used Different PWM Control Techniques”. WSEAS Transactions on Power Systems Vol. 3, 2008. pp 696-703.

[6]. Diaz Rodríguez, J. L., Pabon Fernández, L.D: y Pardo García, A. THD Improvement of a PWM Cascade Multilevel Power Inverters Using Genetic Algorithms as Optimization Method, Wseas Transactions On Power Systems ISSN: 2224-350X, 2015 voumenl:10 fasc: 1 Grecia pages: 46–54.

[7]. T. Sudhakar Babu, K. Priya, D. Maheswaran, K. Sathish Kumar, N. Rajasekar, Selective voltage harmonic elimination in PWM inverter using bacterial foraging algorithm, Swarm and Evolutionary Computation, Volume 20, February 2015, Pages 74-81, ISSN 2210-6502.

[8]. Abdul Moeed Amjad, Zainal Salam, A review of soft computing methods for harmonics elimination PWM for inverters in renewable energy conversion systems, Renewable and Sustainable Energy Reviews, Volume 33, May 2014, Pages 141-153, ISSN 1364-0321, http://dx.doi.org/10.1016/j.rser.2014.01.080.

[9]. Anup Kumar Panda, Yellasiri Suresh, Research on cascade multilevel inverter with single DC source by using three-phase transformers, International Journal of Electrical Power & Energy Systems, Volume 40, Issue 1, September 2012, Pages 9-20, ISSN 0142-0615.

[10]. Malinowski, M.; Gopakumar, K.; Rodriguez, J. and Pérez, M. “A Survey on Cascaded Multilevel Inverters”, IEEE Trans. on Ind. Elect., Vol. 57, N. 7, July 2010, pp. 2197-2206.

[11]. Ilhami Colak, Ersan Kabalci, Ramazan Bayindir, Review of multilevel voltage source inverter topologies and control schemes, Energy Conversion and Management, Volume 52, Issue 2, February 2011, Pages 1114-1128.

[12]. Nayan Kumar, Tapas Kumar Saha, Jayati Dey, Modeling, control and analysis of cascaded inverter based grid-connected photovoltaic system, International Journal of Electrical Power & Energy Systems, Volume 78, June 2016, Pages 165-173, ISSN 0142-0615.

[13]. Venkatachalam Kumar Chinnaiyan, Jovitha Jerome, J. Karpagam, An experimental

investigation on a multilevel inverter for solar energy applications, International Journal of Electrical Power & Energy Systems, Volume 47, May 2013, Pages 157-167, ISSN 0142-0615.

[14]. Bailu Xiao; Lijun Hang; Jun Mei; Riley, C.; Tolbert, L.M.; Ozpineci, B., "Modular Cascaded H-Bridge Multilevel PV Inverter With Distributed MPPT for Grid-Connected Applications," in Industry Applications, IEEE Transactions on , vol.51, no.2, pp.1722-1731, March-April 2015 doi: 10.1109/TIA.2014.2354396.

[15]. Ajami, A.; Farakhor, A.; Ardi, H., "Minimisations of total harmonic distortion in cascaded transformers multilevel inverter by modifying turn ratios of the transformers and input voltage regulation," in Power Electronics, IET , vol.7, no.11, pp.2687-2694, 11 2014 doi: 10.1049/iet-pel.2013.0533.

[16]. Baker R. H. y Lawrence H. B. *Electric Power Converter*, US. Patent Number 3,867,643, 1975.

[17]. Nabae, A., Takahashi, I. and H. Akagi. “A new neutral point clamped PWM inverter”, IEEE Trans. Ins. Appl., vol. IA-17, N. 5, pp.518-523, Sep-Oct, 1981.

[18]. Odeh, C.I., "Improved three-phase, five-level pulse-width modulation switched voltage source inverter," in Power Electronics, IET , vol.8, no.4, pp.524-535, 4 2015 doi: 10.1049/iet-pel.2014.0133.

[19]. Jin-Sung Choi; Feel-Soon Kang, "Seven-Level PWM Inverter Employing Series-Connected Capacitors Paralleled to a Single DC Voltage Source," in Industrial Electronics, IEEE Transactions on , vol.62, no.6, pp.3448-3459, June 2015 doi: 10.1109/TIE.2014.2370948.

[20]. Fengjiang Wu; Xiaoguang Li; Fan Feng; Hoay Beng Gooi, "Modified Cascaded Multilevel Grid-Connected Inverter to Enhance European Efficiency and Several Extended Topologies," in Industrial Informatics, IEEE Transactions on , vol.11, no.6, pp.1358-1365, Dec. 2015, doi: 10.1109/TII.2015.2486623

[21]. L. David Pabón Fernández, E. A. Caicedo y J. L. Díaz Rodríguez, "Comparative analysis of 9 levels cascade multilevel converters with selective harmonic elimination," *Power Electronics and Power Quality Applications (PEPQA), 2015 IEEE Workshop on*, Bogota, 2015, pp. 1-6, doi: 10.1109/PEPQA.2015.7168244.

[22]. Banaei, M. R.; Khounjahan H. and Salary, E. “Single-source cascaded transformers multilevel inverter with reduced number of switches”. IET Power Electron, Vol. 5, N. 9, 2012, pp. 1748- 1753.

[23]. Diaz-Rodríguez, J. L.; Pabón-Fernández, L. D.; Caicedo-Peñaranda, E. A. Novel methodology for the calculation of transformers in power multilevel converters. Ingeniería y competitividad, 2015, vol.17, n. 1.

[24]. T. Sudhakar Babu, K. Priya, D. Maheswaran, K. Sathish Kumar, N. Rajasekar, Selective voltage harmonic elimination in PWM inverter using bacterial foraging algorithm, Swarm and Evolutionary Computation, Volume 20, February 2015, Pages 74-81, ISSN 2210-6502.

[25]. M. Gnana Sundari, M. Rajaram, Sujatha Balaraman, Application of improved firefly algorithm for programmed PWM in multilevel inverter with adjustable DC sources, Applied Soft Computing, Volume 41, April 2016, Pages 169-179, ISSN 1568-4946.

[26]. Debnath, S. Narayan, R. and Ghosh, T. "Comparison of Different Soft Techniques applicable to Multilevel Inverter for Harmonic Elimination". International Journal of Computer Application, Vol. 6, N. 2, Dec., 2012.

[27]. M. Gnana Sundari, M. Rajaram, Sujatha Balaraman, Application of improved firefly algorithm for programmed PWM in multilevel inverter with adjustable DC sources, Applied Soft Computing, V. 41, April 2016, Pages 169-179, ISSN 1568-4946.

[28]. Vivek Kumar Gupta, R. Mahanty, Optimized switching scheme of cascaded H-bridge multilevel inverter using PSO, International Journal of Electrical Power & Energy Systems, Volume 64, January 2015, Pages 699-707.

[29]. IEEE Std. 519-1992-IEEE Recommended Practices and Requirements for Harmonic Control in Electrical Power Systems. IEEE, 1992.

[30]. Diaz-Rodriguez, J. L.; Pabon-Fernandez, L. D. and Contreras-Pena, J. L. Plataforma de bajo costo para la evaluación de fenómenos electromagnéticos monofásicos de calidad de la energía según el estándar IEEE 1159. Dyna rev.fac.nac.minas [online]. 2015, vol.82, n.194 [cited 2016-03-27], pp. 119-129.

[31]. Sánchez, M. A. Calidad de la energía eléctrica. Instituto Tecnológico de Puebla, México, 2009.